

# Comparative Life Cycle Assessment of Neodymium Oxide Electrolysis in Molten Salt


Andrea Schreiber,\* Josefine Marx, Petra Zapp, and Wilhelm Kuckshinrichs

Rare earth elements are used in renewable energy generation techniques like wind turbines as well as in various high-tech applications in the automobile industry, electrical engineering, optics, and catalyzers. Due to the environmentally harmful production of rare earths, they have been subject of life cycle assessment investigations in the past years. Most of these studies focus on rare earth oxide production. The subsequent reduction of rare earth oxides to the final metal in a molten salt electrolysis has significant environmental impacts especially on human toxicity. The main drivers are rare earth fluoride production and molten salt electrolysis. In this study, exemplarily a comparative life cycle assessment of neodymium oxide electrolysis in molten salt as well as various neodymium fluoride production processes is conducted. The different assumptions regarding inputs and outputs of the electrolysis process are discussed. Then, the impacts of the electrolysis processes modeled in different ways are analyzed in relation to the entire process chain to produce neodymium. The results show a share of the electrolysis process on the entire process chain varying from 9% to 82% depending on different assumptions. Based on this analysis, improvements for the electrolysis process are proposed.

## 1. Introduction

Rare earth elements (REEs) are defined as those chemical elements ranging in atomic numbers between 57 and 71 in the periodic table of the elements. REEs are classified into two groups according to their varying ionic radii: light REEs (LREEs) with atomic numbers from 57 (lanthanum) to 62 (samarium) and heavy REEs (HREEs) with atomic numbers from 63 (europium) to 71 (lutetium). Due to their chemical similarity, scandium and yttrium are also part of LREE and HREE, respectively. Neodymium (Nd) is a representative of LREEs.

Dr. A. Schreiber, J. Marx, Dr. P. Zapp, Dr. W. Kuckshinrichs  
Institute of Energy and Climate Research – Systems Analysis and  
Technology Evaluation (IEK-STE)  
Forschungszentrum Jülich  
Wilhelm-Johnen-Straße, Jülich D-52425, Germany  
E-mail: a.schreiber@fz-juelich.de

 The ORCID identification number(s) for the author(s) of this article can be found under <https://doi.org/10.1002/adem.201901206>.

© 2020 The Authors. Published by WILEY-VCH Verlag GmbH & Co. KGaA, Weinheim. This is an open access article under the terms of the Creative Commons Attribution License, which permits use, distribution and reproduction in any medium, provided the original work is properly cited.

DOI: 10.1002/adem.201901206

In 2018, 170 000 t of rare earth oxide (REO) equivalents were produced worldwide, hereof 120 000 t in China, 20 000 t in Australia, and 15 000 t in the United States.<sup>[1]</sup> The Bayan Obo mine in Inner Mongolia is the largest Chinese REE deposit.<sup>[2]</sup> Regarding the total Chinese REO production, the share of Bayan Obo is approximately 57%. The second largest Chinese REE source, especially for HREEs, are ion adsorption clays (IAC) located in the south of China.<sup>[3,4]</sup> IAC deposits account for approximately 37% of Chinese REE production.<sup>[2]</sup> Together with the Bayan Obo mine, they represented approximately 70% of world REO production in 2018. Nd holds a share of approximately 18% on the total REE production.<sup>[5]</sup>

REEs are used in many application areas, especially in magnets for motors and wind turbines (24%).<sup>[6]</sup> In a gearless 3 MW onshore wind turbine, for example, about 2 t of Nd iron boron magnet are needed, containing about 530 kg of Nd and 130 kg of praseodymium.<sup>[7]</sup> Furthermore, REEs

are used in catalysts, polishing powder, battery alloys, glass additives, phosphors, and ceramics as well as in everyday objects such as smartphones, tablets, and hard disks.<sup>[6]</sup>

Due to the high significance of REEs, they have been analyzed in many life cycle assessment (LCA) studies in recent years.<sup>[8–25]</sup> These LCA studies show that REE production is associated with high ecological impacts. Most studies consider the Chinese production up to REOs either from Bayan Obo<sup>[9–12,25]</sup> or from IACs.<sup>[16,18,22,23]</sup> Only five studies broaden the focus and analyze the entire process chain up to RE metal.<sup>[10,14–16,24]</sup>

Today, the final production of RE metals by electrolysis or other reduction processes takes place almost exclusively in China. Molten salt electrolysis (MSE) is the dominating industrial technique to obtain Ce, La, Nd, and Pr, and accounts for 80–90% of RE metal production in China.<sup>[26]</sup> As Nd is the most common RE component in magnets, this study focuses on Nd processing via MSE. However, for Chinese MSE production sites, no primary data are available. Therefore, previous LCA studies have modeled the Chinese MSE using various assumptions, leading to different results.<sup>[10,14–16,24]</sup> The approach in this study uses published life cycle inventories (LCI) of Nd<sub>2</sub>O<sub>3</sub> MSE (in total ten different inventories)<sup>[10,14–16]</sup> and integrates them into the identical Bayan Obo process chain recently published by the authors,<sup>[14]</sup> to examine the effect of MSE on the entire Nd production.

The main drivers of the ecological impacts of MSE are identified by comparing the different LCIs to highlight possible improvements for MSE.

## 2. Production of Nd via Molten Salt Electrolysis

### 2.1. Production of Nd Oxide

The starting material for the production of Nd metal is  $\text{Nd}_2\text{O}_3$ , which can be obtained by different process routes depending on the ore type (bastnaesite, monazite, IAC). **Figure 1** shows the highly simplified process chain for Bayan Obo in China based on a mixed bastnaesite/monazite raw ore. The raw ore is mined in an open pit mining process. The crushed ore is ground to a size of  $<74\ \mu\text{m}$  by conventional wet grinding. Separation of the ferrous magnetite is carried out magnetically. The ore pulp of the magnetic separation passes through a multistage flotation resulting in a mixed bastnaesite and monazite concentrate with 55.6% and 34.1% of REO. After flotation, both concentrates are roasted using sulfuric acid in a rotary kiln. The obtained RE sulfates are leached with water as well as sulfuric acid and afterward filtrated.

By adding water and ammonium bicarbonate, RE carbonates are precipitated. Adding water and hydrochloric acid converts the precipitated RE carbonates into a RE chloride solution. Several solvent extraction steps are necessary to separate single REEs subsequently. The subsequent precipitation is carried out using oxalic acid. The resulting Nd oxalate is calcined to  $\text{Nd}_2\text{O}_3$  in a tunnel furnace at  $900\ ^\circ\text{C}$ .

### 2.2. Production of Nd

RE metals can be processed from REOs using different metal refining processes like metallothermic reduction with calcium or electrolysis processes. Metallothermic reduction must be performed in a batch mode and is very energy intensive due to the high temperatures required. Compared with the metallothermic reduction, MSE consumes less energy and can be conducted as a continuous process. MSE is the dominating industrial technique to obtain Ce, La, Nd, and Pr.<sup>[26]</sup>

The conventional Nd MSE, operated by a 3 kA rectifier, has a cylindrical shape with an internal diameter of 40 cm and a filling bath with a filling level of 35 cm. The melting pot consists of

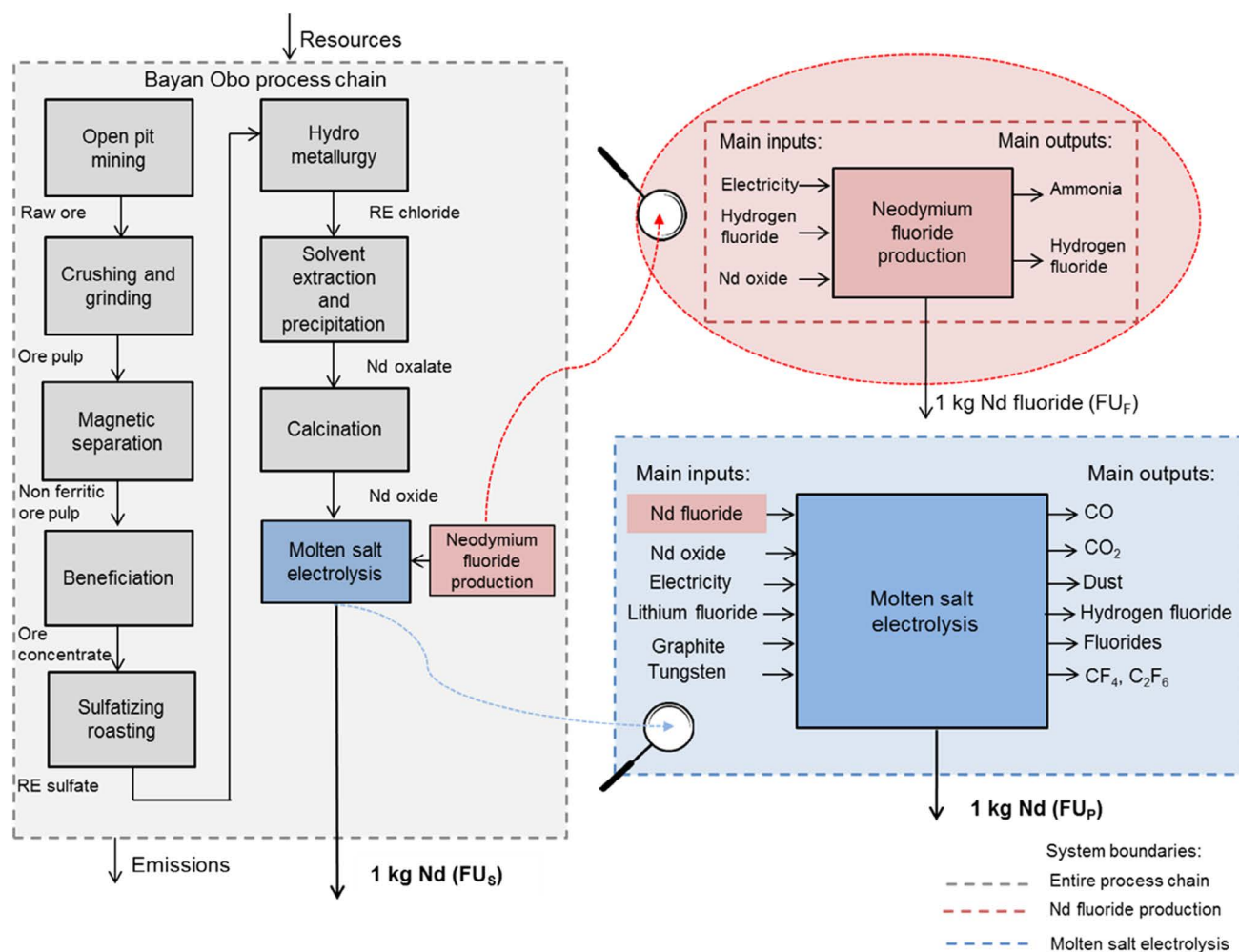


**Figure 1.** Schematic process chain of Bayan Obo (grey) and the single processes of neodymium fluoride production (red) and of molten salt electrolysis (blue) included therein.

graphite, while the collecting pan is made of tungsten (W) or molybdenum (Mo). The collecting pan is located under the cathode at the bottom of the cell, where the refined liquid Nd accumulates. The molten salt electrolyte consists of about 80–90% of Nd fluoride ( $\text{NdF}_3$ ) and 10–20% of lithium fluoride (LiF), in which the  $\text{Nd}_2\text{O}_3$  is dissolved. Tungsten cathode(s) are immersed vertically in the electrolyte and graphite anodes are placed around them. A voltage is applied between anode and cathode and the dissociated  $\text{Nd}^{3+}$  ion at the cathode is reduced to metal. At the graphite anode, the oxygen ions are oxidized to oxygen, which reacts with carbon to carbon monoxide (CO) and carbon dioxide ( $\text{CO}_2$ ). Undesired side reactions can occur, leading to an increased formation of perfluorocarbons (PFCs), which are powerful greenhouse gases.<sup>[27]</sup> The anode is exchanged regularly, which requires the electrolysis process to be stopped. This leads to an instable process with high losses of electrolyte, electricity, and material.<sup>[28]</sup> In addition, this manually controlled process of anode replacement does not encompass any off-gas purification.<sup>[29]</sup>

Due to the high demand for Nd, an improvement of the technique seems mandatory, which would imply higher power capacity, fewer losses of electrolyte, and an adequate process control. Therefore, the power capacity of electrolysis cells was gradually increased. These days, modern large-scale plants in China operate with 30 kA. Changing the anode to four quadrant segments enables the electrolysis to continue production during the exchange of segments, which, in turn, stabilizes the process and raises the efficiency.

Compared with the 3 kA cell, the power requirements of an 8–30 kA cell was reduced from approximately 12 kWh to 8.5 kWh  $\text{kg}^{-1}$  Nd.<sup>[29]</sup> Strict environmental thresholds in China can be met by off-gas collection and purification. Depending on wet or dry exhaust scrubbing systems, dust emissions can be reduced to 90–99% and fluorides to maximally 96%. The dust resulting from dry filtration or the wet scrubber can be processed and  $\text{NdF}_3$ , LiF, and  $\text{Nd}_2\text{O}_3$  can be recycled.<sup>[30]</sup>

### 3. Experimental Section

LCA was a well-established method for a holistic evaluation of environmental effects of a product system considering the entire life cycle and was documented in the ISO 14040/14044 standards.<sup>[31,32]</sup> According to the ISO standards, LCA was subdivided into four steps: 1) goal and scope definition to describe the object, the system boundaries, and the functional unit (FU) of the analysis; 2) life cycle inventory analysis (LCI) to compile material and energy inputs and their subsequent outputs; 3) life cycle impact assessment (LCIA) to evaluate the potential environmental impacts; and 4) interpretation to summarize the results and to draw a conclusion giving recommendations.

LCIA considered issues related to human health, natural environment, and resource use. The emissions and resources compiled in LCI were assigned to so-called impact categories. This raised the question of how to compare impact categories that did not measure the same thing (e.g., global warming and human toxicity). Therefore, the ISO 14040/14044 standards provided an optional step called normalization. Normalization was a way to examine the importance and the magnitude of impact categories in relation to a reference system. The results

of each impact category were divided by a selected reference, which put all the results on the same scale.<sup>[33]</sup> In addition, the normalized impacts became dimensionless. For example, the reference can be 1) the total inputs and outputs for a given geographical area over a given reference year (e.g., the impact of the European Union for 2010); 2) the total inputs and outputs for a given geographical area over a given reference year on a per capita basis (e.g., the impact of a European citizen in 2010).<sup>[33]</sup> The results will be easier to understand when compared with the environmental impact of a geographical area or a single person over a year.<sup>[33]</sup>

To evaluate the environmental burdens in this study, the impact assessment method “CML 2001–Jan. 2016” was chosen.<sup>[34]</sup> CML 2001 was developed by the Institute of Environmental Sciences at the Leiden University, The Netherlands. The following impact categories were included in the assessment: Abiotic Depletion<sub>fossil</sub> (FD) [MJ], Acidification Potential (AP) [kg  $\text{SO}_2$  eq.], Eutrophication Potential (EP) [kg Phosphate eq.], Global Warming Potential (GWP 100 years) [kg  $\text{CO}_2$  eq.], Photochemical Ozone Creation Potential (POCP) [kg Ethene eq.], Human Toxicity Potential (HTP) [kg DCB eq.], and an adapted Abiotic Depletion<sub>elementary</sub> (ADP) [kg Sb eq.]. Despite the high criticality, no resource indicator of any LCIA methods covered individual REEs appropriately so far. Therefore, new characterization factors (CFs) for 15 REEs and some other metals (e.g., iron, aluminum, and chromium) were estimated by Adibi et al.<sup>[35]</sup> To develop the CFs, Adibi et al. collected a wide range of data from U.S. Geological Survey (USGS) and other mining reports for 11 large REE deposits. We included these new CFs for the REEs in the CML resource depletion indicator ADP. Thus, our analysis also included the evaluation of the REEs within the adapted ADP (Figure 2 and 3).

For normalization, the reference system “CML2001–Jan. 2016, World, year 2000, incl biogenic carbon”, which represents the world impacts in the year 2000, was chosen. Unfortunately, there were still no normalization factors (appropriate reference system) for the new REE CFs. Therefore, ADP cannot be normalized (Figure 4, 5, and 6).

#### 3.1. Goal and Scope

This study focused on MSE of  $\text{Nd}_2\text{O}_3$ . As no primary data were available for MSE, previous LCA studies by Sprecher et al.,<sup>[10]</sup> Zhao et al.,<sup>[15]</sup> Lee and Wen,<sup>[16]</sup> Vahidi et al.,<sup>[24]</sup> and Schreiber et al.<sup>[14]</sup> had modeled the Chinese electrolysis process using different assumptions, e.g., regarding the state of the art. In this article, the proposed electrolysis processes were compared. Based on the studies by Sprecher et al.,<sup>[10]</sup> Zhao et al.,<sup>[15]</sup> Lee and Wen,<sup>[16]</sup> (three electrolysis scenarios: best, middle, worst), and Schreiber et al.<sup>[14]</sup> (four electrolysis scenarios: best, middle, worst, average), nine electrolysis processes were modeled and compared using GaBi software version 9.2.0.58 by Thinkstep<sup>[36]</sup> (Table 1). In addition to these nine electrolysis processes, a future electrolysis process was established for the year 2030 to show improvement potentials. Therefore, Schreiber et al.’s best scenario (Table 1) was selected, but with less tungsten and a Chinese electricity mix for 2030.<sup>[37]</sup>

We did not consider the study by Vahidi et al.<sup>[24]</sup> even though they provided LCI data for  $\text{Nd}_2\text{O}_3$  MSE for different facilities, too.

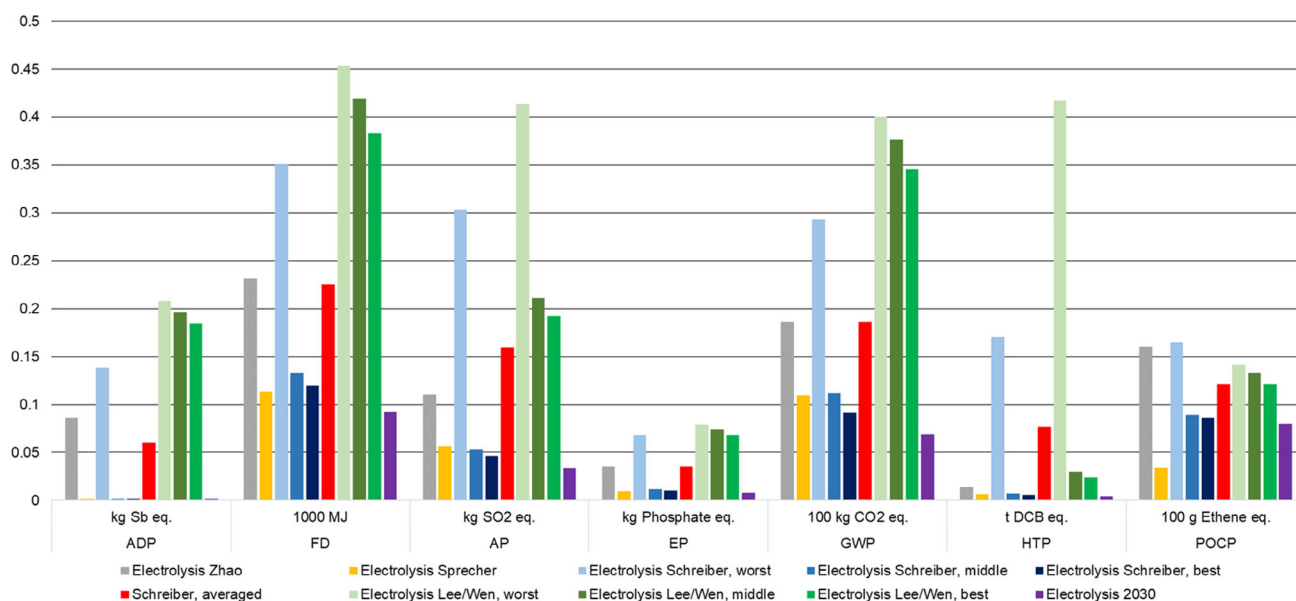


**Figure 2.** Life cycle impacts during production of 1 kg Nd via MSE ( $FU_P$ ).

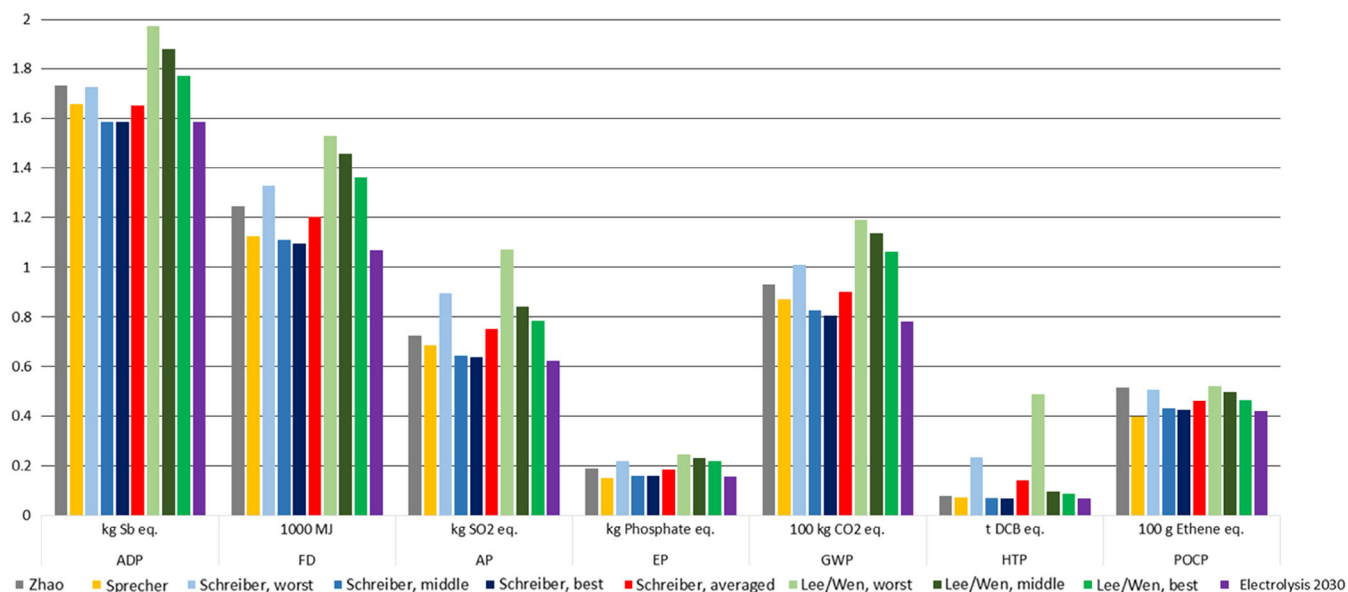


**Figure 3.** Life cycle impacts to produce 1 kg of Nd along the entire process chain ( $FU_S$ ).

The reason for this was the economic-based allocation method used, which was based on different production baskets (various metals) of the facilities. By allocating the single-output  $Nd_2O_3$  MSE process with respect to price for all products of the entire facility, the environmental life cycle impacts of Nd differed. In case Nd was produced in a facility along with REEs of high economic value, Nd's environmental impact was lower than in case REEs of lower economic value were produced along with Nd. This made no sense as, in fact,  $Nd_2O_3$  MSE was no multi-output process, and thus Nd production had a certain environmental impact regardless of other REEs' economic value.

For the 10 modeled electrolysis processes, the different amounts of inputs—e.g.,  $NdF_3$ , graphite, tungsten, LiF, refractory material, and electricity from the mentioned LCA studies—were used and modeled in the GaBi software. These required inputs were then supplemented using an individual upstream process for each from the ecoinvent 3.5 database, except for  $NdF_3$ . For  $NdF_3$  supply, the same approach as for electrolysis was used. Based on the studies by Schreiber et al.,<sup>[14]</sup> Zhao et al.,<sup>[15]</sup> and Lee and Wen,<sup>[16]</sup> five different  $NdF_3$  production processes were modeled in GaBi: one for Zhao et al.,<sup>[15]</sup> one for Schreiber et al.,<sup>[14]</sup> and three for Lee and Wen<sup>[16]</sup> (Table 1).

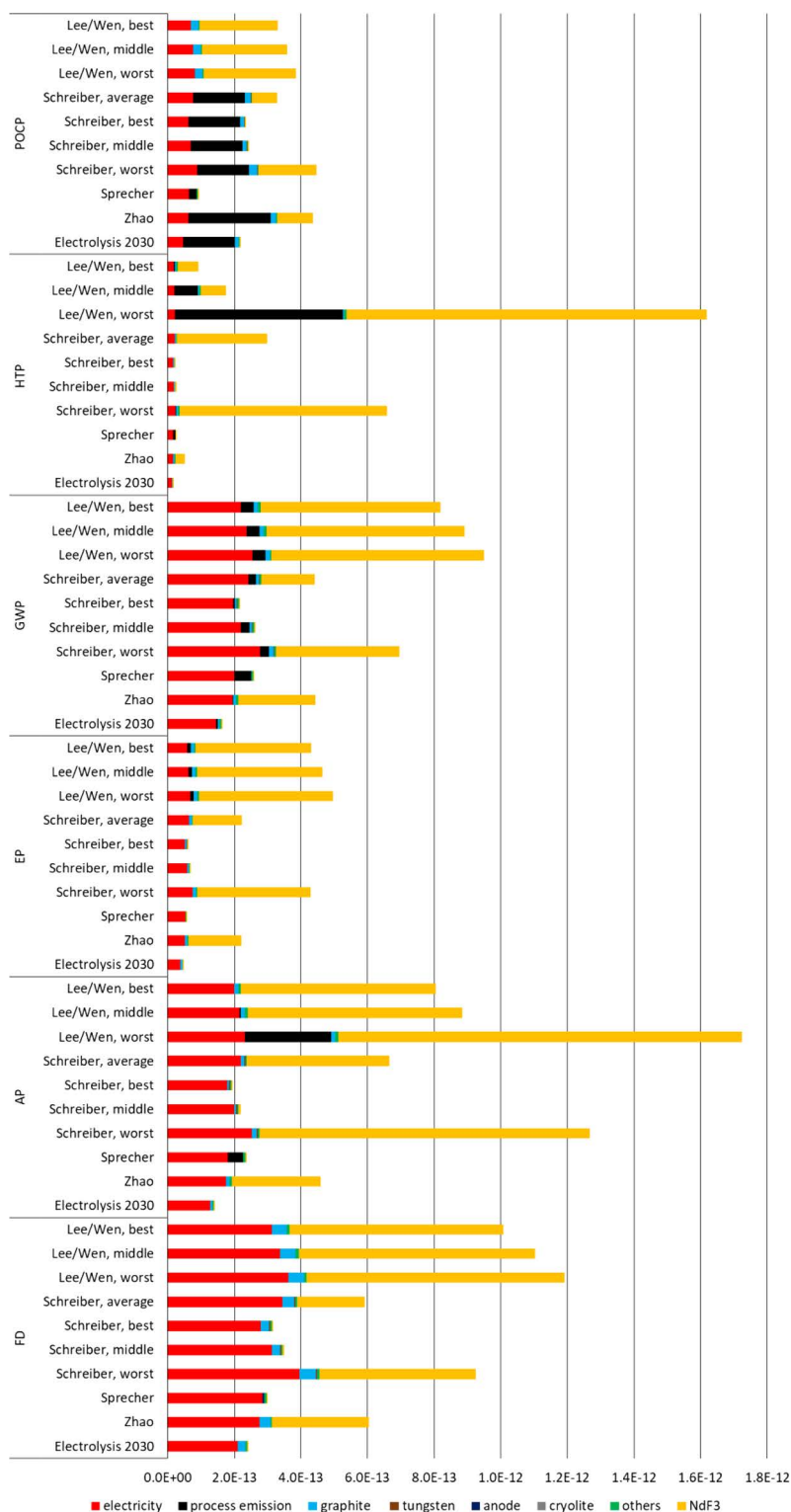


**Figure 4.** Life cycle impacts (normalized) to produce 1 kg Nd via MSE (FU<sub>p</sub>).

These NdF<sub>3</sub> processes were then integrated into the corresponding electrolysis inventories. Schreiber et al.'s<sup>[14]</sup> NdF<sub>3</sub> production applied to all of their electrolysis inventories. Sprecher et al.<sup>[10]</sup> did not use NdF<sub>3</sub>.

Each electrolysis inventory was then integrated in the identical, recently published LCA of the Nd<sub>2</sub>O<sub>3</sub> Bayan Obo process chain.<sup>[14]</sup> All upstream operations such as mining of the raw ore, beneficiation, roasting, chemical treatment, solvent

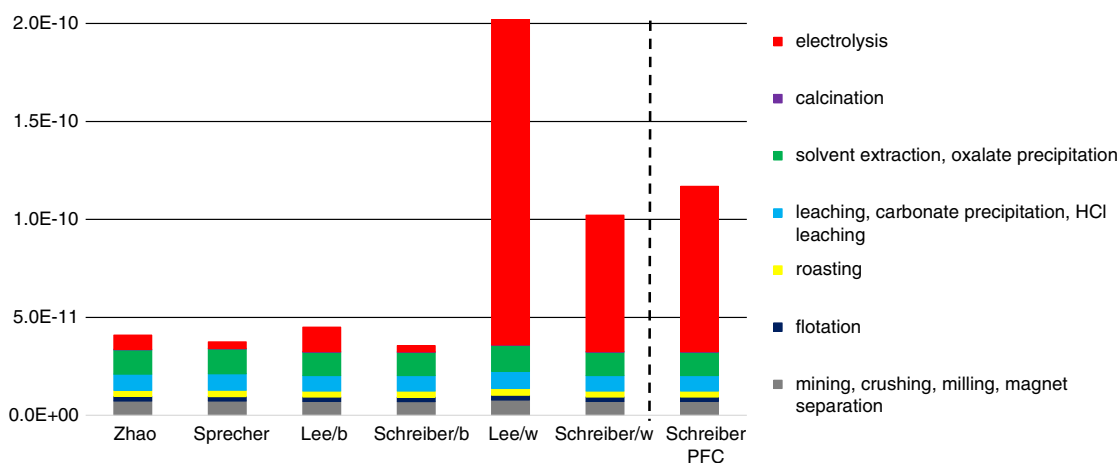


**Figure 5.** Life cycle impacts (normalized) to produce 1 kg Nd along selected process chains ( $FU_S$ ) subdivided into process chain segments.

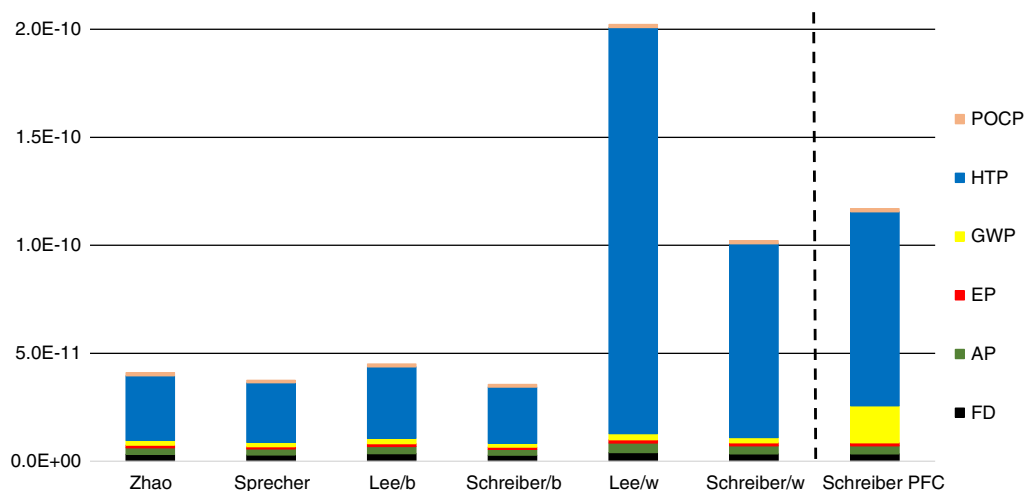


**Figure 6.** Life cycle impacts (normalized) to produce 1 kg Nd along selected process chains ( $FU_S$ ) subdivided into different impact categories.

extraction, and calcination as well as transports, waste disposal, and energy supply were included within the system boundary (Figure 1). The  $Nd_2O_3$  Bayan Obo process chain remained the same for all assessments to show the impacts of the different MSE explicitly. Electricity was provided by the Chinese electricity mix from 2014 and was used for all analyses except for “Electrolysis scenario 2030.” The electricity mix 2014 comprised hard coal to 72.5%, hydroelectricity to 18.6%, wind power to 2.73%, nuclear power to 2.32%, natural gas to 2.16%, bioenergy to 0.78%, photovoltaics to 0.51%, energy from waste to 0.23%, oil to 0.17%, and geothermal energy to 0.002%.<sup>[38]</sup> For the “Electrolysis scenario 2030,” a Chinese electricity mix forecast 2030 with less hard coal and more natural gas, wind power, nuclear power, and photovoltaics was used: hard coal, 49.15%; hydroelectricity, 14.57%; wind power, 9.43%; nuclear power, 7.91%; natural gas, 7.57%; bio energy, 2.72%; photovoltaics, 8.57%; oil, 0.05%; geothermal energy, 0.03%.<sup>[36]</sup> For all power generation techniques,ecoinvent 3.5 processes were used.

To quantify the environmental burdens of the MSE as a single process, 1 kg of Nd was chosen as the functional unit of the

process ( $FU_P$ ) (Figure 1). The intermediate results of  $NdF_3$  production were related to the functional unit of 1 kg of  $NdF_3$  ( $FU_F$ ) (Figure 1). For the calculation of the entire Nd production system, the functional unit ( $FU_S$ ) was 1 kg of Nd, which had passed through the entire process chain from raw ore mining to electrolysis (Figure 1).

## 3.2. Life Cycle Inventory Analysis

### 3.2.1. $NdF_3$ Production

Table 1 shows the LCI data for  $NdF_3$  production related to the  $FU_F$ .  $NdF_3$  can be produced in different ways.<sup>[39]</sup> Schreiber et al.<sup>[14]</sup> described an  $NdF_3$  production based on Spedding and Dane’s<sup>[38]</sup> process where ammonium hydrogen fluoride was used to convert REO into RE fluoride. Resulting emissions were the decomposition products ammonia and hydrogen fluoride (HF). Lee and Wen<sup>[16]</sup> assumed a direct fluorination process, where HF passed through the REO at high temperatures, which explained the higher electricity consumption.

**Table 1.** Inventories of NdF<sub>3</sub> production (FU<sub>F</sub> 1 kg NdF<sub>3</sub>) and Nd<sub>2</sub>O<sub>3</sub> MSE (FU<sub>P</sub> 1 kg Nd).

	Unit	Zhao <sup>[15]</sup>	Sprecher <sup>[10]</sup>	Lee <sup>[16]</sup> best	Lee <sup>[16]</sup> middle	Lee <sup>[16]</sup> worst	Schreiber <sup>[14]</sup> worst	Schreiber <sup>[14]</sup> middle	Schreiber <sup>[14]</sup> best	Schreiber <sup>[14]</sup> average	Electrolysis 2030
Inputs of NdF <sub>3</sub> production related to 1 kg NdF <sub>3</sub>											
Electricity	kWh	0.528	–	5	10	15	0.336	0.336	0.336	0.336	0.336
Hydrogen fluoride	kg	0.331	–	0.609	0.761	0.913	0.741	0.741	0.741	0.741	0.741
Neodymium oxide	kg	0.755	–	0.919	0.944	0.97	0.880	0.880	0.880	0.880	0.880
Ammonia	kg		–				0.306	0.306	0.306	0.306	0.306
Water, deionized	kg	1.51	–	8	8	8					
Transport, lorry	tkm		–	0.184	0.189	0.194	0.038	0.038	0.038	0.038	0.038
Transport, rail	tkm		–	0.735	0.755	0.776					
Outputs of NdF <sub>3</sub> production related to 1 kg NdF <sub>3</sub>											
Neodymium oxide	kg		–				0.044	0.044	0.044	0.044	0.044
Ammonia	kg		–	2.00E–04	2.00E–04	2.00E–04	0.354	0.354	0.354	0.354	0.354
Hydrogen fluoride <sup>a)</sup>	kg	2.50E–04	–	1.25E–03	6.47E–03	0.609	0.477	0.477	0.477	0.477	0.477
Hydrogen fluoride <sup>b)</sup>	kg	0.393	–								
Arsenic <sup>c)</sup>	kg			2.40E–06	2.40E–06	2.40E–06					
Cadmium <sup>c)</sup>	kg			6.40E–07	6.40E–07	6.40E–07					
COD <sup>c,d)</sup>	kg			6.40E–04	6.40E–04	6.40E–04					
Chloride <sup>a)</sup>	kg			8.93E–03	8.93E–03	8.93E–03					
Chromium <sup>c)</sup>	kg			8.00E–06	8.00E–06	8.00E–06					
Chromium (+VI) <sup>c)</sup>	kg			2.40E–06	2.40E–06	2.40E–06					
Dust <sup>a)</sup>	kg			0.0107	0.0107	0.0107					
Fluoride <sup>c)</sup>	kg			8.00E–05	1.70E–04	1.70E–04					
Fluorspar, 97% purity	kg			0.805	1.2						
Hydrochloric acid <sup>a)</sup>	kg			0.0143	0.0143	0.0143					
Lead <sup>c)</sup>	kg			4.00E–06	4.00E–06	4.00E–06					
Nitrogen <sup>c)</sup>	kg			4.00E–04	4.00E–04	4.00E–04					
Nitrous oxide <sup>a)</sup>	kg			0.0357	0.0357	0.0357					
Oil <sup>a)</sup>	kg			4.00E–05	4.00E–05	4.00E–05					
Phosphorus <sup>c)</sup>	kg			2.40E–05	2.40E–05	2.40E–05					
Solids <sup>c)</sup>	kg			5.60E–04	1.60E–03	1.60E–03					
Thorium <sup>c)</sup>	kg			8.00E–07	8.00E–07	8.00E–07					
Thorium <sup>a)</sup>	kg			1.80E–05	1.80E–05	1.80E–05					
Zinc <sup>c)</sup>	kg			1.20E–05	1.20E–05	1.20E–05					
Waste water	kg						0.134	0.134	0.134	0.134	0.134
Inputs of electrolysis related to 1 kg Nd											
Electricity	kWh	8.38	8.62	9.5	10.3	11	12.	9.5	8.5	10.4	8.5
Graphite	kg	0.186		0.25	0.26	0.27	0.285	0.135	0.135	0.2	0.135
Lithium fluoride	kg	8.00E–03		0.01	0.0125	0.015	0.01	7.04E–04	6.53E–04	4.70E–03	6.53E–04
Tungsten	kg	2.50E–04					2.70E–03	2.70E–03	2.70E–03	2.70E–03	2.70E–04
Neodymium oxide	kg	1.17	1.2	1.15	1.2	1.25	1.13	1.13	1.13	1.13	1.13
Neodymium fluoride	kg	0.08		0.14	0.145	0.15	0.11	1.10E–03	5.76E–04	0.048	5.76E–04
Steel, unalloyed	kg	3.00E–03									
Water, deionized	kg	42.9		8	8	8					
Refractory	kg	0.0275	7.00E–04				0.09	0.09	0.09	0.09	0.09
Sodium hydroxide, 50%	kg	2.50E–04									
Quicklime	kg	2.50E–03							2.43E–04	3.40E–05	2.34E–04
Calcium hydroxide	kg			1.65E–01	1.79E–01						

**Table 1.** Continued.

	Unit	Zhao <sup>[15]</sup>	Sprecher <sup>[10]</sup>	Lee <sup>[16]</sup> best	Lee <sup>[16]</sup> middle	Lee <sup>[16]</sup> worst	Schreiber <sup>[14]</sup> worst	Schreiber <sup>[14]</sup> middle	Schreiber <sup>[14]</sup> best	Schreiber <sup>[14]</sup> average	Electrolysis 2030
Disposal, inert waste	kg		4.14E−03				0.12	0.12	0.12	0.12	0.12
Disposal, bitumen	kg		7.56E−04								
Cryolite	kg		1.41E−03								
Heavy fuel oil	MJ		1.125								
Al electrolysis, plant	unit		9.70E−11								
Aluminum fluoride	kg		0.0118								
Disposal, filter dust	kg		1.26E−03								
Anode, Al electrolysis	kg		8.50E−02								
Cathode, Al electrolysis	kg		3.42E−03								
Disposal, refractory	kg		1.20E−03								
Rock wool	kg		1.10E−04								
Chlorine, liquid	kg		1.00E−04								
Nitrogen, liquid	kg		6.00E−04								
MG-silicon	kg		0.0108								
Argon, liquid	kg		1.50E−03								
Palm oil	kg		8.00E−05								
Corrugated board	kg		1.80E−03								
Al casting plant	unit		1.54E−10								
Disposal, dross from Al electrolysis	kg		1.10E−04								
Water	kg								1.25	0.175	1.25
Transport, lorry	tkm	1.03 <sup>(c)</sup>	0.05	0.23	0.24	0.25	0.26	0.137	0.137	0.19	0.135
Transport, rail	tkm		0.88	0.92	0.96	1					
Outputs of electrolysis related to 1 kg Nd											
Calcium fluoride	kg			0.074	0.076						
CO <sub>2</sub>	kg	0.1112	0.283	0.294	0.307	0.32	0.055	0.055	0.055	0.055	0.055
CO	kg	0.336	0.0173				0.211	0.211	0.211	0.211	0.211
SO <sub>2</sub>	kg		8.35E−03								
NO <sub>x</sub>	kg		6.04E−05								
Hydrogen fluoride	kg		5.25E−04	1.75E−04	6.25E−04	0.0457	1.02E−04			4.39E−05	
C <sub>2</sub> F <sub>6</sub>	g		2.65E−05				0.014 (12 <sup>f</sup> )	0.014	0.0014	0.0118	0.0014
CF <sub>4</sub>	g		0.238				0.14 (74 <sup>f</sup> )	0.14	0.014	0.118	0.014
PAH <sup>(g)</sup>	kg		4.32E−05								
Benzo(a)pyrene	kg		1.23E−06								
Fluoride <sup>(c)</sup>	kg	2.00E−04		8.00E−05	8.00E−05	8.00E−05					
Particulates, 2.5 µm	kg						0.12	5.35E−04	6.27 E-05	5.18E−02	6.27E−05
Particulates, <2.5 µm	kg	1.00E−05	2.46E−03								
Particulates, 2.5–10 µm	kg	2.30E−03	0.61E−04								
Carbon	kg						0.18	0.03	0.03	0.095	0.03
Suspended solids <sup>(c)</sup>	kg			5.60E−04	1.60E−03	1.60E−03					
Unspecified oils <sup>(c)</sup>	kg			4.00E−05	4.00E−05	4.00E−05					
COD <sup>(d)</sup>	kg			6.40E−04	6.40E−04	6.40E−04					
Total phosphorous <sup>(c)</sup>	kg			2.40E−05	2.40E−05	2.40E−05					
Total nitrogen <sup>(c)</sup>	kg			4.00E−04	4.00E−04	4.00E−04					
Ammonia <sup>(c)</sup>	kg			2.00E−04	2.00E−04	2.00E−04					



**Table 1.** Continued.

	Unit	Zhao <sup>[15]</sup>	Sprecher <sup>[10]</sup>	Lee <sup>[16]</sup> best	Lee <sup>[16]</sup> middle	Lee <sup>[16]</sup> worst	Schreiber <sup>[14]</sup> worst	Schreiber <sup>[14]</sup> middle	Schreiber <sup>[14]</sup> best	Schreiber <sup>[14]</sup> average	Electrolysis 2030
Total zinc <sup>c)</sup>	kg			1.20E−05	1.20E−05	1.20E−05					
Thorium <sup>c)</sup>	kg			8.00E−07	8.00E−07	8.00E−07					
Cadmium <sup>c)</sup>	kg			6.40E−07	6.40E−07	6.40E−07					
Lead <sup>c)</sup>	kg			4.00E−06	4.00E−06	4.00E−06					
Arsenic <sup>c)</sup>	kg			2.40E−06	2.40E−06	2.40E−06					
Chromium <sup>c)</sup>	kg			8.00E−06	8.00E−06	8.00E−06					
Chromium (VI) <sup>c)</sup>	kg			2.40E−06	2.40E−06	2.40E−06					
Particulate dust	kg			1.50E−03	1.50E−03	1.50E−03					
Chloride <sup>a)</sup>	kg			1.25E−03	1.25E−03	1.25E−03					
Hydrochloric acid <sup>a)</sup>	kg			2.00E−03	2.00E−03	2.00E−03					
Nitrous oxide <sup>a)</sup>	kg			5.00E−03	5.00E−03	5.00E−03					
Thorium <sup>a)</sup>	kg			3.00E−06	3.00E−03	3.00E−03					
Heat, waste	MJ		14.7								
Water	kg		4.71						1.25	0.175	1.25
Waste for disposal	kg						2.00E−03	2.00E−03	8.00E−03	2.84E−03	8.00E−03

<sup>a)</sup>Emission into air; <sup>b)</sup>By-product HF, 20% solution; <sup>c)</sup>Emission into water; <sup>d)</sup>COD = Chemical oxygen demand; <sup>e)</sup>Assumed transport distances from Schreiber;<sup>[14]</sup>  
<sup>f)</sup>Values in brackets are for the scenario: Schreiber, worst/CF<sub>4</sub>, C<sub>2</sub>F<sub>6</sub> emissions based on Vogel and Friedrich;<sup>[27]</sup> <sup>g)</sup>PAH = polycyclic aromatic hydrocarbons.

Lee and Wen<sup>[16]</sup> specified three NdF<sub>3</sub> production scenarios called Lee, worst (Lee/w), Lee, middle (Lee/m), and Lee, best (Lee/b) (Table 1), which differed significantly in HF input and HF emissions. A description of these process variants was not given. Additional emissions reported by Lee and Wen<sup>[16]</sup> were taken from the Emission Standards of Pollutants from RE Industry (MEP)<sup>[40]</sup> but cannot be explained by the inputs. For example, Lee and Wen<sup>[16]</sup> specified ammonium emissions, although no ammonium was added to the process. Zhao et al.<sup>[15]</sup> took the inputs from an Environmental Impact Report of a Chinese facility,<sup>[41]</sup> as published by Vahidi et al.<sup>[24]</sup> Zhao et al.<sup>[15]</sup> also suggested direct fluorination, but with much lower electricity requirements compared with Lee and Wen.<sup>[16]</sup> Schreiber et al.<sup>[14]</sup> assumed that all reaction products and unreacted inputs were transported by the hot off-gas stream as emissions to air. On the contrary, Zhao et al.<sup>[15]</sup> stated that the emitted HF emissions were washed out via water spray adsorption, resulting in a by-product of 20% HF aqueous solution. In addition, Zhao et al.<sup>[15]</sup> calculated a stoichiometric reaction, while the other studies calculated hyperstoichiometric NdF<sub>3</sub> production. Overall, Zhao et al.<sup>[15]</sup> estimated that HF emissions were less than 0.1% of their input.

### 3.2.2. Molten Salt Electrolysis

The second part of Table 1 shows the LCI data of Nd<sub>2</sub>O<sub>3</sub> MSE related to the FU<sub>p</sub>. Although Lee and Wen,<sup>[16]</sup> Zhao et al.,<sup>[15]</sup> and Schreiber et al.<sup>[14]</sup> analyzed the same electrolysis process, there were clear differences that can be attributed to the data sources used and to the different production standards assumed. The electrolysis inventory of Sprecher et al.<sup>[10]</sup> was very different from the others. They adapted data from the Hall–Héroult

electrolysis process, which was utilized for aluminum production, under consideration of different molecular properties.

Schreiber et al.<sup>[14]</sup> had investigated four process options (Schreiber, worst = Schreiber/w; Schreiber, middle = Schreiber/m; Schreiber, best = Schreiber/b; and Schreiber, averaged = Schreiber/av) regarding different material requirements and emissions on the basis of Cheng and Bao.<sup>[42,43]</sup> The worst option represented small, mostly private (backyard) production sites with the outdated 3–4 kA technique without off-gas cleaning and recycling. The middle option, representing the 8 kA technique, was already equipped with dry off-gas cleaning and waste recycling. In the best option, large-scale production sites up to 30 kA with modern process control, wet off-gas cleaning, and recycling were analyzed. In addition, Schreiber/w, Schreiber/m, and Schreiber/b options were considered to build an averaged, more realistic Chinese scenario (Schreiber/av). As no production capacities for the worst, middle, and best options were available, their capacities were estimated as follows. The officially published Nd metal production amounted to approximately 25 000 t in 2010.<sup>[44]</sup> In addition, there was a considerable amount of illegally mined rare earths.<sup>[45–47]</sup> In 2015, for example, already approximately 5850 t of Nd were produced illegally in just two southern provinces.<sup>[45]</sup> As no precise information was available, the amount of illegally produced Nd was estimated to approximately 10 000 t year<sup>−1</sup>. This resulted in an estimated total production of 35 000 t in China. Although the number of backyard production sites decreased significantly in recent years due to governmental shut downs, the share of facilities without off-gas cleaning was still high and was estimated at 15 000 t year<sup>−1</sup> (Schreiber/w). As electrolysis had been further developed in China, it was assumed that all large facilities were equipped with off-gas cleaning, but only a few with electronic

process optimization technique.<sup>[29]</sup> Therefore, the remaining amount of 20 000 t was distributed to Schreiber/m (15 000 t) and Schreiber/b (5000 t). Data for the inventories were based on literature research with support of experts from the Institute of Metallurgy at RWTH Aachen University.

Lee and Wen<sup>[16]</sup> also analyzed three electrolysis scenarios (Lee/w, Lee/m, and Lee/b) to account for large discrepancies in efficiency and waste treatment. The inventory was based on an industry survey and a study from Pang.<sup>[26]</sup> The worst scenario represented small- to medium-sized enterprises with low capacity and minimal or no waste treatment. The best scenario represented high capacity enterprises with latest technology and waste treatment to meet environmental standards. The average scenario modeled the Chinese mean for efficiency and waste treatment. However, the difference between the best and worst scenario in terms of technology and environmental standards was not reflected in the inventory data. With the exception of HF emissions, there were no significant differences (Table 1).

Zhao et al.<sup>[15]</sup> used data from an environmental report of a large Chinese facility, which produced approximately 2000 t year<sup>-1</sup>.<sup>[41]</sup> The use of quicklime indicated the installation of a wet air scrubber, thus this facility was comparable with the best options of Schreiber et al.<sup>[14]</sup> and Lee and Wen.<sup>[16]</sup>

### 3.2.3. Inputs to the Nd Molten Salt Electrolysis

The energy requirement for electrolysis depended on the technology used. The difference between modern technology and outdated 3 kV technique was approximately 40%.

The graphite demand for the anode was between 0.105 and 0.255 kg kg<sup>-1</sup> Nd. The lowest value in Schreiber/m, Schreiber/b, and Electrolysis 2030 represented graphite recycling. As the cathode was not consumed, the demand for tungsten was very low. In Schreiber et al.,<sup>[14]</sup> the cathode consumption was calculated on the basis of the geometry and an estimated replacement interval of 2 years. It added up to 2.7 g tungsten g<sup>-1</sup> Nd, and was more than 10 times higher than in Zhao et al.<sup>[15]</sup> The LCI of tungsten was based on the Chinese production pathway analyzed by Lu et al.<sup>[48]</sup> and covered more than 80% of the worldwide tungsten production. Lee and Wen<sup>[16]</sup> did not consider any cathode material.

The inputs of the electrolyte materials LiF and NdF<sub>3</sub> were very different. The NdF<sub>3</sub> input was between 0.57 and 150 g kg<sup>-1</sup> Nd. Even the best options of Schreiber et al.<sup>[14]</sup> and Lee and Wen<sup>[16]</sup> differed by factor 240. In contrast, in the worst options of Schreiber et al.<sup>[14]</sup> and Lee and Wen,<sup>[16]</sup> the NdF<sub>3</sub> input was similar with 0.15 and 0.11 kg kg<sup>-1</sup> Nd, respectively. In Schreiber/w, the value was based on the outdated 3 kV technology from Bao.<sup>[43]</sup> The very low electrolyte requirement in Schreiber's middle and best option was based on Cheng,<sup>[42]</sup> representing better process techniques with less electrolyte losses and higher efficiency of the off-gas cleaning system. In addition, LiF and NdF<sub>3</sub> were recycled.<sup>[29]</sup> In Lee and Wen,<sup>[16]</sup> there were only minor differences between the worst, middle, and best option, although the techniques assumed were different, just the LiF demand differed.

As the equipment required for Nd electrolysis was low, only a few materials were considered. In addition to the anode material, Zhao et al.<sup>[15]</sup> and Schreiber et al.<sup>[14]</sup> also included refractory

material. The holders of the anode blocks were neglected by Schreiber et al.<sup>[14]</sup> and Lee and Wen<sup>[16]</sup> and accounted for 3 g steel kg<sup>-1</sup> Nd in Zhao et al.<sup>[15]</sup> In Schreiber et al.,<sup>[14]</sup> the melting pot, which also consisted of graphite, was included in the inventory (30 g kg<sup>-1</sup> Nd). The quantity was estimated based on the geometry and the lifetime assumed. Lee and Wen<sup>[16]</sup> did not consider any other materials.

The inventory of Sprecher et al.<sup>[10]</sup> showed no major differences regarding energy consumption and Nd<sub>2</sub>O<sub>3</sub> requirement. However, cryolite and aluminum fluoride were used as electrolytes instead of LiF and NdF<sub>3</sub>. Moreover, anode and cathode material from aluminum electrolysis were considered. For the anode, petrol coke and pitch were used instead of graphite. For the cathode, carbon blocks were used instead of tungsten.

### 3.2.4. Emissions of Nd Molten Salt Electrolysis

The reported emissions differed strongly in the individual studies. As Lee and Wen<sup>[16]</sup> used the Chinese discharge standards,<sup>[39]</sup> they indicated emissions like hydrochloric acid and NO<sub>x</sub> that cannot be caused by electrolysis.

Furthermore, CO<sub>2</sub> emissions differed considerably between the studies. They were approximately 6 and 2 times higher in Lee and Wen<sup>[16]</sup> and Zhao et al.<sup>[15]</sup> than those of Schreiber et al.<sup>[14]</sup> (Table 1). However, Lee and Wen<sup>[16]</sup> did not report CO emissions in contrast to Zhao et al.,<sup>[15]</sup> Schreiber et al.,<sup>[14]</sup> and Sprecher et al.<sup>[10]</sup> It was reasonable to assume that Lee and Wen<sup>[16]</sup> considered the reaction of CO with atmospheric oxygen to CO<sub>2</sub> and therefore reported the highest CO<sub>2</sub> emissions. If the conversion of CO to CO<sub>2</sub> had also been assumed in Schreiber et al.,<sup>[14]</sup> the CO<sub>2</sub> emissions would have been similar. The CO<sub>2</sub> emissions given in Schreiber et al.<sup>[14]</sup> were calculated according to the mass balance of the MSE on the basis of Bao and Liu.<sup>[43,49]</sup>

The emissions of fluoride and their compounds were also carried out differently. HF emissions were only considered in Lee and Wen,<sup>[16]</sup> Schreiber/w, as well as in Sprecher et al.<sup>[10]</sup> and varied between 0.1 g kg<sup>-1</sup> Nd (Schreiber/w) and 46 g kg<sup>-1</sup> Nd (Lee/w). The HF emissions in Schreiber/w were roughly estimated on the mass balance for wet scrubbing.<sup>[42]</sup> For Schreiber's middle and best options, it was assumed that HF was filtered or washed out from the off gas.

In addition to HF emissions into air, Zhao et al.<sup>[15]</sup> and Lee and Wen<sup>[16]</sup> indicated fluoride emissions into water. Schreiber et al.<sup>[14]</sup> considered the decomposition of the electrolyte (LiF, NdF<sub>3</sub>) as dust emissions. For backyard facilities without exhaust air filtration, dust emissions amounted to 120 g kg<sup>-1</sup> Nd and for modern plants with dust filtration to 0.06 g kg<sup>-1</sup> Nd. In other studies, dust emissions were between 1.5 and 3.1 g kg<sup>-1</sup> Nd and thus significantly higher than in Schreiber/m as well as Schreiber/b. In addition to dust filtering, a further reason was the lower NdF<sub>3</sub> and LiF use in these scenarios. In contrast to Schreiber et al.,<sup>[14]</sup> Lee and Wen<sup>[16]</sup> did not consider the different technical facility standards and reported the same dust value for all scenarios.

Sprecher et al.<sup>[10]</sup> also considered other emissions such as nitrogen oxide, sulfur dioxide, benzopyrene, and PAHs, which were all based on the aluminum production process from the ecoinvent database.<sup>[50]</sup>

PFC emissions were only taken into account by Schreiber et al.<sup>[14]</sup> and Sprecher et al.<sup>[10]</sup> although they had a high climate-damaging effect. As no published data were available for PFC emissions for industrial MSE of REOs, Schreiber et al.<sup>[14]</sup> estimated CF<sub>4</sub> emissions of 0.135 g kg<sup>-1</sup> Nd on the basis of aluminum electrolysis for Schreiber/w and Schreiber/m. For C<sub>2</sub>F<sub>6</sub>, 10% of the CF<sub>4</sub> value was assumed. In the Schreiber/b scenario, PFC emissions were significantly reduced under the assumption of an automated process.

## 4. Results of the Life Cycle Impact Assessment

Table 2 shows the impact scores of 1 kg of NdF<sub>3</sub> production (FU<sub>F</sub>), 1 kg of Nd metal production via MSE analyzed as a single

process (FU<sub>P</sub>), and 1 kg of Nd metal production along the entire Bayan Obo process chain (FU<sub>S</sub>).

### 4.1. Nd Fluoride Production

Looking at the impact scores for NdF<sub>3</sub> production individually, Zhao et al.<sup>[15]</sup> have the lowest impact across all impact categories. The reason lies in the fact that they have the smallest input of Nd<sub>2</sub>O<sub>3</sub>, low energy consumption, and a low amount of HF input. In addition, they have the lowest HF emissions that cause HTP. The highest HTP impact was found for Lee/w followed by Schreiber et al.<sup>[14]</sup> due to the highest HF emissions. The highest value for AP is found in Schreiber et al.,<sup>[14]</sup> caused by additional ammonia emissions due to the different NdF<sub>3</sub> manufacturing process. The significantly higher energy input (up to 44 times

**Table 2.** Life cycle impacts to produce 1 kg of NdF<sub>3</sub> (FU<sub>F</sub>), 1 kg of Nd (FU<sub>P</sub>) via MSE, and 1 kg of Nd along the entire process chain (FU<sub>S</sub>).

	ADP [kg Sb eq.]	FD [MJ]	AP [kg SO <sub>2</sub> eq.]	EP [kg Phosphate eq.]	GWP [kg CO <sub>2</sub> eq.]	HTP [kg DCB eq.]	POCP [g Ethene eq.]
Per kg NdF <sub>3</sub>							
Zhao <sup>[15]</sup>	1.08	1370	0.793	0.308	121	86.3	48.9
Schreiber <sup>[14]</sup>	1.26	1620	2.15	0.485	141	1460	57.5
Lee, worst <sup>[16]</sup>	1.39	1960	1.93	0.422	179	1850	67.4
Lee, middle <sup>[16]</sup>	1.35	1860	1.06	0.407	172	132	64.7
Lee, best <sup>[16]</sup>	1.31	1740	0.996	0.391	162	111	61.4
Per kg Nd via molten salt electrolysis							
Zhao <sup>[15]</sup>	0.0862	231	0.110	0.0348	18.6	13.2	16.0
Sprecher <sup>[10]</sup>	0.00168	113	0.0561	0.00895	10.9	6.37	3.4
Schreiber, worst <sup>[14]</sup>	0.138	351	0.303	0.0676	29.3	170	16.4
Schreiber, middle <sup>[14]</sup>	0.00078	132	0.0522	0.0108	11.1	6.75	8.89
Schreiber, best <sup>[14]</sup>	0.000125	119	0.0461	0.00956	9.07	5.45	8.59
Schreiber, averaged <sup>[14]</sup>	0.0598	225	0.159	0.035	18.6	76.7	12.1
Lee, worst <sup>[16]</sup>	0.191	453	0.413	0.0783	40	417	14.1
Lee, middle <sup>[16]</sup>	0.178	419	0.211	0.0732	37.6	29.1	13.2
Lee, best <sup>[16]</sup>	0.165	383	0.192	0.068	34.5	23.5	12.1
Electrolysis 2030	0.000136	91.4	0.0331	0.00795	6.85	4.21	7.95
Sensitivity PFC <sup>a)</sup>	0.138	351	0.303	0.0676	652	170	16.4
Per kg Nd along the entire process chain							
Zhao <sup>[15]</sup>	1.73	1244	0.722	0.189	92.7	77.2	51.3
Sprecher <sup>[10]</sup>	0.561	1122	0.684	0.150	86.8	71.2	39.6
Schreiber, worst <sup>[14]</sup>	1.73	1330	0.894	0.216	100.9	231.6	50.5
Schreiber, middle <sup>[14]</sup>	1.58	1110	0.642	0.159	82.4	68.3	42.9
Schreiber, best <sup>[14]</sup>	1.58	1094	0.636	0.158	80.3	67.0	42.6
Schreiber, averaged <sup>[14]</sup>	1.65	1200	0.750	0.183	90.0	138	46.1
Lee, worst <sup>[16]</sup>	0.780	1530	1.07	0.243	119	485	51.9
Lee, middle <sup>[16]</sup>	0.743	1458	0.840	0.231	113.5	94.6	49.4
Lee, best <sup>[16]</sup>	0.697	1361	0.784	0.217	106.1	85.2	46.3
Electrolysis 2030	1.58	1066	0.623	0.155	78.1	65.7	41.9
Sensitivity PFC <sup>a)</sup>	1.73	1330	0.894	0.216	723.6	231.6	50.5

<sup>a)</sup>Results of the sensitivity analysis described in Section 4.4.

higher) in Lee and Wen<sup>[16]</sup> is hardly reflected in FD and GWP because most is caused by the upstream  $\text{Nd}_2\text{O}_3$  production, which is a major input in the  $\text{NdF}_3$  production (Table 1) and modeled alike for all, based on Schreiber et al.<sup>[14]</sup>

#### 4.2. Molten Salt Electrolysis

Figure 2 shows the impact scores of the 10 electrolysis processes, which differ in their inventories, as described in Sections 2.2 and 3.2.2 To show all values in one figure, some numbers had to be multiplied or divided by factors (10, 100, and 1000). Thus, the scales of units in Figure 2 are different (g, kg, t). Here, the scores of Lee/w are highest with exception of POCP, mainly caused by the highest amount of  $\text{NdF}_3$  input per kg Nd produced. Almost 100% of ADP are caused by RE ore extraction for  $\text{NdF}_3$  production in case of Schreiber's, Lee's, and Zhao's analyses due to the new REE CFs in the impact method. Sprecher et al.<sup>[10]</sup> and the "Electrolysis scenario 2030" have the lowest impacts. The main reason for the lower figures in Sprecher et al.<sup>[10]</sup> is the use of  $\text{AlF}_3$  instead of  $\text{NdF}_3$ . In addition, Sprecher et al.<sup>[10]</sup> indicate the lowest HF emissions. For the "Electrolysis scenario 2030," lower tungsten consumption (factor 10 compared with Schreiber/b) and a more ecological electricity mix (−23% hard coal compared to 2014) result in lower impacts compared with Schreiber/b, especially reflected in FD, GWP, and AP.

An overview of environmental impacts (normalized) with their causally associated inputs during electrolysis is shown in Figure 4. It must be noted that all HTP values are divided by 100 because they are very high in case of Schreiber/w and Lee/w so that all impacts can be shown in a diagram. In the case of Sprecher et al.,<sup>[10]</sup> the yellow bar does not represent  $\text{NdF}_3$ , but  $\text{AlF}_3$  as mentioned before.

The high contribution of  $\text{NdF}_3$  to all impacts is clearly visible. Therefore, Lee and Wen<sup>[16]</sup> and Schreiber/w score highest due to the large  $\text{NdF}_3$  input. Due to an assumed  $\text{NdF}_3$  recycling and better process control during electrolysis in the case of Schreiber/m and Schreiber/b, the impacts caused by  $\text{NdF}_3$  are hardly visible anymore.

Only Zhao et al.<sup>[15]</sup> and Schreiber et al.<sup>[14]</sup> consider CO emissions, which are visible as direct process emissions in POCP (Figure 4). If CO converts to  $\text{CO}_2$  with atmospheric oxygen, POCP will decrease and GWP will increase.

HTP is mainly generated by HF emissions. Lee/w scores worst because of the HF emissions ( $45 \text{ g HF kg}^{-1} \text{ Nd}$ ), which are the highest by far compared, for example, with Sprecher et al.<sup>[10]</sup> ( $0.5 \text{ g HF kg}^{-1} \text{ Nd}$ ) and Schreiber/w ( $0.1 \text{ g HF kg}^{-1} \text{ Nd}$ ). In Schreiber/m, Schreiber/b, Zhao et al.,<sup>[15]</sup> and "Electrolysis scenario 2030," no HF emissions are assumed. In the case of Sprecher et al.,<sup>[10]</sup> AP is induced by direct sulfur dioxide emissions ( $\text{SO}_2$  does not occur in any other study) and in the case of Lee/w by high HF emissions. Sprecher et al.'s impact assessment is hardly comparable to other studies because his electrolysis process is based on aluminum electrolysis.<sup>[10]</sup>

The environmental impacts generated by electricity consumption differ not very much between the studies because electricity consumption lies in the same order of magnitude for all of them (approximately  $8\text{--}12 \text{ kWh kg}^{-1} \text{ Nd}$ ). Furthermore, in all analyses we used the same Chinese electricity mix. The direct  $\text{CO}_2$

emissions during electrolysis are negligible as  $\text{CO}_2$  emissions from electricity generation are significantly higher. GWP is also caused by  $\text{CF}_4$  and  $\text{C}_2\text{F}_6$ , which are typical MSE emissions. However, only Sprecher et al.<sup>[10]</sup> and Schreiber et al.<sup>[14]</sup> consider PFCs (maximum  $0.24 \text{ g CF}_4$ , maximum  $0.027 \text{ g C}_2\text{F}_6$ ), which are estimated from aluminum electrolysis. Looking at the direct process emissions, the share of  $\text{CF}_4$ ,  $\text{C}_2\text{F}_6$ , and  $\text{CO}_2$  on the total GWP amounts to 60%, 10%, and 30% for Schreiber/w and Schreiber/m and changes to 16%, 3%, and 81% for Schreiber/b. The importance of PFC emissions decreases when looking at the improved electrolysis processes, and even more so when looking at the entire process chain.

#### 4.3. Entire Process Chain

Figure 3 shows the impact scores to produce 1 kg of Nd along the entire Bayan Obo process chain (Figure 1). As shown in Figure 2, the scales of units have to be adjusted to display all numbers in one figure. The pattern of impact distribution of the entire process chain (Figure 3) looks similar to the one of the single-process MSE (Figure 2). However, as expected, the impacts are higher for the entire process chain than those of the single electrolysis process (Figure 2) due to Bayan Obo's upstream processes like mining, roasting and solvent extraction. Lee/w and Schreiber/w do not stick out as much anymore, especially for FD, AP, and GWP. Again, almost 100% of ADP is caused by RE ore extraction used for  $\text{NdF}_3$  and  $\text{Nd}_2\text{O}_3$  production. As the Sprecher et al.'s process chain<sup>[10]</sup> also uses  $\text{Nd}_2\text{O}_3$  from Bayan Obo, Sprecher's ADP of the entire process chain is in the same order of magnitude as the other ADP values.

To show the share of the MSE process on the entire process chain, the environmental impacts are added. To enable this, the different impacts are normalized and are therefore dimensionless (see Section 3). In Figure 5 and 6, the normalized life cycle impacts to produce 1 kg of Nd along the entire process chain ( $\text{FU}_s$ ) are presented. For the worst and best scenarios, the process chains are subdivided into seven process chain segments (Figure 5) and six impact categories (Figure 6). The first six segments from mining to calcination describe the production of  $\text{Nd}_2\text{O}_3$ . The top red bars show the impacts of electrolysis. The share of electrolysis on the total environmental impacts to produce 1 kg of Nd rises from 9% in Schreiber/b and Sprecher et al.,<sup>[10,14]</sup> over 18% in Zhao et al.,<sup>[15]</sup> 28% in Lee/b, 68% in Schreiber/w up to 82% in Lee/w.

The high share of electrolysis in the case of Schreiber/w and Lee/w is mainly caused by high HF emissions during  $\text{NdF}_3$  production and electrolysis.

The calcination of RE oxalates to REOs induced the lowest environmental impacts, followed by flotation, roasting, mining–magnetic separation, leaching, and solvent extraction. According to our approach, only the share of the electrolysis process differs between the studies. As already shown in the evaluation of the single electrolysis processes, Sprecher et al.'s and Schreiber/b's electrolysis contributes the least,<sup>[10,14]</sup> followed by Zhao's electrolysis, Lee/b's, Schreiber/w's, and Lee/w's, which has by far the largest share of the process chain.

The pattern of impact distribution is shown in Figure 6 and is the same in all studies. This is not surprising as all analyses are

based on the same Bayan Obo process chain published by Schreiber et al.,<sup>[14]</sup> except for  $\text{NdF}_3$  production and the electrolysis process. The normalization step shows the dominant contribution of HTP to the overall impacts. The other impacts are evenly spread. As mentioned earlier, HF emissions during  $\text{NdF}_3$  production and direct HF emissions during MSE mainly cause HTP. The main reason for HTP in the other process chain segments is heavy metals and PAH emissions, which are produced by various upstream and downstream processes (e.g., electricity generation, waste disposal, and production of chemicals and tungsten).

#### 4.4. Sensitivity Analysis

In a recently published experimental study, Vogel and Friedrich prove considerable tetrafluoromethane ( $\text{CF}_4$ ) and hexafluoroethane ( $\text{C}_2\text{F}_6$ ) emissions by rare earth electrolysis, if no process control is installed.<sup>[27]</sup> Their laboratory measurements of  $\text{CF}_4$  and  $\text{C}_2\text{F}_6$  in the off gas confirmed the possibility of continuous PFC emission of about 74 g  $\text{CF}_4$  and 12 g  $\text{C}_2\text{F}_6$   $\text{kg}^{-1}$  Nd.<sup>[27]</sup> These measurements are taken for a sensitivity analysis (called sensitivity PFC). All other assumptions in sensitivity PFC are based on Schreiber/w (Table 1). By raising the  $\text{CF}_4$  and  $\text{C}_2\text{F}_6$  emissions from 0.14 g  $\text{CF}_4$   $\text{kg}^{-1}$  Nd and 0.014 g  $\text{C}_2\text{F}_6$   $\text{kg}^{-1}$  Nd in the electrolysis of Schreiber/w to 74 g  $\text{CF}_4$  and 12 g  $\text{C}_2\text{F}_6$   $\text{kg}^{-1}$  Nd measured by Vogel and Friedrich<sup>[27]</sup>, GWP increases by a factor of 22 for 1 kg Nd produced via MSE ( $\text{FU}_p$ ) (Table 2). Looking at the entire process chain, the normalized GWP increases by a factor of 7 for 1 kg Nd produced along the entire process chain ( $\text{FU}_s$ ) (Figure 6). A reason for this is the high  $\text{CO}_2$  equivalents of  $\text{CF}_4$  (7390  $\text{CO}_2$ -eq.  $\text{kg}^{-1}$ ) and  $\text{C}_2\text{F}_6$  (12 200  $\text{CO}_2$ -eq.  $\text{kg}^{-1}$ ). The share of electrolysis on the total environmental impacts to produce 1 kg of Nd rises up to 72% (Figure 5).

## 5. Conclusion

This study compared the environmental performances of ten MSE processes. Due to the lack of primary data, the electrolysis process had to be modeled based on several assumptions. The electrolysis LCI data were gathered from own analyses as well as published studies and were supplemented with the same upstream and downstream processes. Furthermore, the different electrolysis processes were linked to a recently published process chain to produce  $\text{Nd}_2\text{O}_3$  from the Chinese Bayan Obo raw ore to investigate the importance of the electrolysis on the entire Nd production.

Although the electrolysis processes model the same technology type, there are large differences in the environmental impacts according to their assumptions. One significant difference lies within the description of production standards (backyard facilities with 3–4, 8, or 30 kA plants, off-gas cleaning). No individual process description shows a representative overall scenario for China, but only possible production variants. Although the average scenario prepared by Schreiber et al.<sup>[14]</sup> comprises large uncertainties, e.g., regarding the estimated amounts of illegal mining, it is the first attempt to describe an overall Chinese electrolysis situation.

Overall, the share of MSE on the total environmental impact of Nd production varies between 9% and 82%, mainly depending on production standards and assumptions made about emissions. Data about emissions bear high uncertainty, as no on-site measured data are available, just thresholds. Especially the assumptions for  $\text{NdF}_3$  production have a high impact on the importance of the MSE process in total.

The comparison for the different processes revealed that HF emissions during  $\text{NdF}_3$  production and as direct emissions during MSE are a large driver for the overall environmental performance. At the same time, however, they are also subject to the greatest uncertainty. For example, Zhao et al.<sup>[15]</sup> used data from an environmental report of a Chinese RE factory. Yet, the report does not consider any HF emissions at all. The emissions specified by Lee and Wen<sup>[16]</sup> are based on Chinese threshold values. It is also unclear how much of the HF emissions are released into air and how much into water. The CML 2001 – Jan. 2016 impact assessment method used in this study assesses HF emissions to air or water differently, which is an additional cause of uncertainty. However, the figures for Schreiber/w and Schreiber/b reveal the effect of HF reduction by off-gas cleaning very clearly.

Uncertainties also exist with regard to PFC emissions. Sprecher et al.<sup>[10]</sup> and Schreiber et al.<sup>[14]</sup> estimated PFC emissions in analogy to aluminum electrolysis data, while Lee and Wen and Zhao et al. consider no PFCs at all. But even the assumed PFC values in Sprecher et al.<sup>[10]</sup> and Schreiber et al.<sup>[14]</sup> seem to underestimate the problem considerably, as recently published experimental measurements of significantly higher PFC suggests.<sup>[27]</sup> The effect on GWP was shown in a sensitivity analysis. To get a more precise view, direct off-gas measurements at the electrolysis sites are needed. This emphasizes the importance of automated process control, which should reduce the unregulated production of PFC emissions.

The results have also shown a high influence of  $\text{NdF}_3$  on the environmental impacts. The amount of LiF and  $\text{NdF}_3$  used in electrolysis could be reduced considerably by dust filter and recycling.

In contrast, the electricity consumption cannot be reduced significantly because a voltage reduction would lead to a lower energy input into the electrolysis cell and thus to a disturbance of the heat balance. Lower environmental impacts can only be achieved by more sustainable electricity generation.

Automated process control, off-gas cleaning, and recycling can offer a large potential for optimization. All of these measures would lead to a significant reduction of the environmental burden for Nd production and have potential to be industrially optimized.

The comparison of MSE in different studies has shown the high sensitivity of assumptions regarding production standards and emissions. This clearly indicates that the results must be handled with care, if no reliable data from Chinese RE production are available.

## Conflict of Interest

The authors declare no conflict of interest.

## Keywords

life cycle assessment, molten salt electrolysis, neodymium, rare earth elements

Received: October 7, 2019

Revised: January 14, 2020

Published online:

- [1] D. Bernhardt, J. F. Reilly, *Mineral Commodity Summaries 2019: U.S. Geological Survey*, Vol. 2019, U.S. Government Publishing Office, Washington, DC **2019**, p. 200.
- [2] D. Schüler, M. Buchert, L. Ran, S. Dittrich, C. Merz, *Study on Rare Earth and Their Recycling*, Öko-Institut, Darmstadt **2011**.
- [3] Y. Kanazawa, M. Kamitani, *J. Alloys Compd.* **2006**, 408–412, 1339.
- [4] X. J. Yang, A. Lin, X.-L. Li, Y. Wu, W. Zhou, Z. Chen, *Environ. Dev.* **2013**, 8, 131.
- [5] S. Glöser-Chahoud, A. Kühn, L. Terceroespinoza, *Working Paper Sustainability and Innovation*, No. S05/2016, Fraunhofer ISI, Karlsruhe **2016**.
- [6] R. Bade, *Rare Earths Review—Is the Hype Justified?* Libertas Capital Corporate Finance Limited, London **2010**.
- [7] A. Schreiber, J. Marx, P. Zapp, *J. Cleaner Prod.* **2019**, 233, 561.
- [8] J. E. Zhang, C. Can, *Inst. Min.* **2013**, 4, 38.
- [9] P. Koltun, A. Tharumarajah, *ISRN Metall.* **2014**, 2014, 10.
- [10] B. Sprecher, Y. Xiao, A. Walton, J. Speight, R. Harris, R. Kleijn, G. Visser, G. J. Kramer, *Environ. Sci. Technol.* **2014**, 48, 3951.
- [11] P. Nuss, M. J. Eckelman, *PLoS ONE* **2014**, 9, e101298.
- [12] G. G. Zaines, B. J. Hubler, S. Wang, V. Khanna, *ACS Sustainable Chem. Eng.* **2015**, 3, 237.
- [13] A. Schreiber, J. Marx, P. Zapp, J.-F. Hake, D. Voßenkaul, B. Friedrich, *Resources* **2016**, 5, 32.
- [14] J. Marx, A. Schreiber, P. Zapp, F. Walachowicz, *ACS Sustainable Chem. Eng.* **2018**, 6, 5858.
- [15] P. S. Arshi, E. Vahidi, F. Zhao, *ACS Sustainable Chem. Eng.* **2018**, 6, 3311.
- [16] J. C. K. Lee, Z. Wen, *J. Ind. Ecol.* **2017**, 21, 1277.
- [17] J. Navarro, F. Zhao, *Front. Energy Res.* **2014**, 2.
- [18] E. Vahidi, J. Navarro, F. Zhao, *Resour. Conserv. Recycl.* **2016**, 113, 1.
- [19] C. Browning, S. Northey, N. Haque, W. Bruckard, M. Cooksey, *Rewas 2016: Towards Materials Resource Sustainability*, John Wiley & Sons, Inc., Hoboken, NJ **2016**, 81.
- [20] N. Adibi, Z. Lafhaj, E. D. Gemechu, G. Sonnemann, J. Payet, *J. Rare Earths* **2014**, 32, 288.
- [21] N. Haque, A. Hughes, S. Lim, C. Vernon, *Resources* **2014**, 3, 614.
- [22] R. Schulze, F. Lartigue-Peyrou, J. Ding, L. Schebek, M. Buchert, *J. Sustainable Metall.* **2017**, 3, 753.
- [23] P. Zapp, J. Marx, A. Schreiber, B. Friedrich, D. Voßenkaul, *Resour. Conserv. Recycl.* **2018**, 130, 248.
- [24] E. Vahidi, F. Zhao, *Resour. Conserv. Recycl.* **2018**, 139, 178.
- [25] H. J. Althaus, M. Chudacoff, R. Hirschier, N. Jungbluth, M. Osses, A. Primas, *Lifecycle Inventories of Chemicals. Phosphate Rock. Final Report Ecoinvent Data V 2.0 No.8*, EMPA Dübendorf, Swiss Centre for Life Cycle Inventories, Dübendorf **2007**.
- [26] S. Pang, *Chin. J. Rare Met.* **2011**, 35, 440.
- [27] H. Vogel, B. Friedrich, *Light Metals* (Ed: O. Martin), Springer International Publishing, Cham, Switzerland **2018**, p. 1507.
- [28] S. Fu, *Chin. Rare Earth* **2007**, 28, 45.
- [29] H. W. H. Vogel, *Prozessoptimierung Der Neodym-Schmelzflusselektrolyse Zur Verringerung Von Treibhausgasemissionen*, RWTH Aachen University, Aachen, **2018**.
- [30] Y. Ou, C. Zhou, *Jiangxi Nonferrous Met.* **2006**, 20, 33.
- [31] International Organization for Standardization (ISO), *ISO 14040: Environmental Management—Life Cycle Assessment—Principles and Framework*, **2006**.
- [32] International Organization for Standardization (ISO), *ISO 14044: Environmental Management—Life Cycle Assessment—Requirements and Guidelines*, **2006**.
- [33] V. Aymard, V. Botta-Genoulaz, *Supply Chain Forum Int. J.* **2017**, 18, 76.
- [34] J. B. Guinée, M. Gorée, R. Heijungs, G. Huppes, R. Kleijn, A. d. Koning, L. v. Oers, A. Wegener Sleeswijk, S. Suh, H. A. Udo de Haes, H. D. Bruijn, R. V. Duin, M. A. J. Huijbregts, *Handbook on Life Cycle Assessment. Operational Guide to the ISO Standards. I: LCA in Perspective. IIa: Guide. IIb: Operational Annex. III: Scientific Background*, Kluwer Academic Publishers, Dordrecht **2002**.
- [35] N. Adibi, Z. Lafhaj, J. Payet, *Int. J. Life Cycle Assess.* **2019**, 24, 712.
- [36] thinkstep AG, *thinkstep*, thinkstep AG, Leinfelden-Echterdingen **2019**.
- [37] IEA, *World Energy Outlook 2018*, International Energy Agency, Paris, **2018**.
- [38] IEA, *World Energy Outlook 2014*, International Energy Agency, Paris, **2014**.
- [39] C. K. Gupta, N. Krishnamurthy, *Extractive Metallurgy of Rare Earths*, CRC Press, Boca Raton **2005**.
- [40] MEP, Ministry of Environmental Protection, Beijing **2011**.
- [41] Jiangxi Taihe New Materials Limited, *Environmental Impact Report for Jiangxi Taihe New Materials Limited (in Chinese)*, China Ruilin Engineering Technology Co., Ltd., Nanchang **2016**.
- [42] Y. Cheng, Y. Liang, D. Tao, *Chin. Rare Earth* **2011**, 32, 92.
- [43] J. Bao, *Rare Met. Lett.* **2004**, 23, 35.
- [44] MIIT, *Ministry of Industry and Information Technology*, **2014**.
- [45] R. Nguyen, D. Imholte, *JOM* **2016**, 68, 1948.
- [46] J. Wübbeke, *Resources Policy* **2013**, 38, 384.
- [47] D. J. Packey, D. Kingsnorth, *Resources Policy* **2016**, 48, 112.
- [48] K. Lu, X. Gong, B. Sun, Q. Ding, *Mater. Sci. Forum* **2019**, 1137.
- [49] K. Liu, *Chin. J. Nonferrous Met.* **2001**, 11, 1118.
- [50] M. Classen, H. J. Althaus, S. Blaser, W. Scharnhorst, M. Tuchschild, G. Doka, N. Jungbluth, M. F. Emmenegger, *Life Cycle Inventories of Metals. Part I Aluminium. Final Report Ecoinvent Data V2.0 No 10* EMPA Dübendorf, Swiss Centre for Life Cycle Inventories, Dübendorf **2007**.